Performance Analysis of Highway Vehicle Tracking Using Different Object Trackers

Conference Paper · September 2024

DOI: 10.1109/PEEIACON63629.2024.10800074

5 authors, including:

Md. Sumsur Rahman Shanto
Rajshahi University of Engineering and Technology

Sm Muhtashin Al Razi
Rajshahi University of Engineering and Technology

Md. Selim Hossain
Rajshahi University of Engineering and Technology

Sheikh Shafaet Islam
Rajshahi University of Engineering and Technology

2024 IEEE International Conference on Power, Electrical, Electronics and Industrial Applications (PEEIACON)
12-13 September, RUET, Rajshahi, Bangladesh

Performance Analysis of Highway Vehicle Tracking Using Different Object Trackers

Md. Sumsur Rahman Shanto[1], SM Muhtashin Al Razi[2], Md. Selim Hossain[3], Sheikh Shafaet Islam[4], and Md. Maniruz Zaman[5]
Department of Electrical and Electronic Engineering (EEE)
Rajshahi University of Engineering & Technology (RUET), Rajshahi-6204, Bangladesh[1,2,3,4,5]
Eastern University, Bangladesh[1], Uttara University, Bangladesh[5]
Email: shantoruet18@gmail.com[1], muhtashin99@gmail.com[2], prof.selim@eee.ruet.ac.bd[3], shafaet.niloy21@gmail.com[4], and mmzaman.ruet@gmail.com[5]

***Abstract*— Radar is a crucial technology widely used across various sectors, including the military, defense, space exploration, environmental monitoring, and traffic control. This paper presents advancements in radar technology, focusing on extended object tracking and multipath radar reflections to enhance tracking and classification accuracy in challenging environments such as heavy rain, fog, and dense traffic. We explore two main systems: the first employs parametric variation in object tracking to reduce false alarms and errors, significantly improving the tracking performance. The second system leverages multipath radar reflections, where parametric adjustments have led to a notable increase in target detection accuracy (91.42%). This improvement is particularly vital for applications requiring precise target identification, such as autonomous driving and vehicle tracking, ensuring safer and more efficient operations. Our results demonstrate the effectiveness of parametric modeling in optimizing radar systems for better reliability and robustness in diverse applications. This research contributes to the development of safer transportation systems and more accurate environmental sensing, showcasing the potential of advanced radar technologies in addressing real-world challenges.**

Keywords—Doppler Effect, Object Tracker, GGIW-PHD Tracker, GM-PHD Tracker, Occlusion Analysis.

I. Introduction

The burgeoning concern over sound highways and transportation systems highlights the urgent need to address increasing road accidents caused by adverse weather conditions like storms, rain, fog, and intense sunlight. These accidents often result in substantial losses of time, life, and property. Advanced radar and video-based tracking systems have emerged as critical solutions to mitigate these risks by enabling precise vehicle movement tracking and speed detection, thus enhancing traffic management and safety.

Recent studies emphasize the significance of video capture and processing systems in traffic surveillance. These systems not only assess vehicle speeds but also provide valuable data for accident prevention strategies [1], [2]. Given the rising incidence of traffic-related fatalities, which remain a leading cause of death globally, the World Health Organization underscores the need for robust traffic management systems that can mitigate these risks [3], [4]. Advancements in machine vision have revolutionized vehicle tracking technologies. Modern systems now feature enhanced detection capabilities that minimize errors and false positives, crucial for managing high-traffic areas and complex traffic scenarios [5]. Despite the advancements, the challenge of achieving uniform accuracy across different devices persists, highlighting a common obstacle for traffic researchers and system developers [6], [7]. The role of extended object tracking and multipath radar reflections in improving classification accuracy and tracking performance is also noteworthy. These technologies facilitate the development of more reliable driver assistance systems and contribute to safer navigation and traffic management [8], [9]. Additionally, the application of parametric variations in tracking algorithms has been shown to significantly enhance detection and tracking accuracy, proving essential for dynamic environments like urban traffic and autonomous driving applications [10]. Innovative approaches, such as employing machine learning algorithms for distinguishing between genuine and false detections in automotive radar sensors, further illustrate the technological progress in this field. These methods address complex scenarios, including multipath effects, which are particularly challenging in cluttered environments [11], [12]. Furthermore, the use of deep neural networks and traditional feature extraction techniques in vehicle detection systems has enabled more precise tracking and categorization of vehicles, improving the overall effectiveness of traffic monitoring systems [2], [13]. These systems are integral to applications like automatic number plate recognition (ANPR), which play a crucial role in enforcing traffic laws and regulations.

Previous studies on vehicle tracking and traffic monitoring have encountered key limitations, particularly in distinguishing between genuine and ghost radar detections, which impact the accuracy of vehicle speed and range measurements. The complexity of reducing false and redundant tracks in dense traffic and errors in vehicle positioning, velocity, and yaw angle estimation due to sensor inaccuracies and environmental factors also pose significant challenges. Additionally, enhancing system robustness in adverse weather conditions has been problematic due to increased sensor noise and reduced visibility. This study aims to address these challenges by refining detection techniques to accurately eliminate ghost effects, employing advanced algorithms to reduce false and redundant tracks, and using sophisticated filtering to improve vehicle state estimates. The proposed model is also planned to increase the robustness of tracking systems in adverse weather through adaptive sensing and robust statistical methods. Overall, this research seeks to enhance traffic flow monitoring and accident prevention, offering potential improvements over traditional methods in traffic management and safety.

II. System Design

A. System Modeling

The proposed system model, shown in fig. 1, comprises several interconnected stages aimed at refining raw radar detections into robust target tracks in dynamic highway

979-8-3315-1798-4/24/$31.00 ©2024 IEEE

2024 IEEE International Conference on Power, Electrical, Electronics and Industrial Applications (PEEIACON) | 979-8-3315-1798-4/24/$31.00 ©2024 IEEE | DOI: 10.1109/PEEIACON63629.2024.10800074

environments. Initially, the Doppler analysis stage processes two primary inputs: raw radar detections and odometry data from the ego car. Leveraging Doppler information from detections and potential motion data from odometry, this stage categorizes detections into dynamic and static categories. Dynamic detections, indicative of moving targets, exhibit discernible Doppler signatures, while static detections, likely representing stationary objects or clutter, display minimal relative velocity.

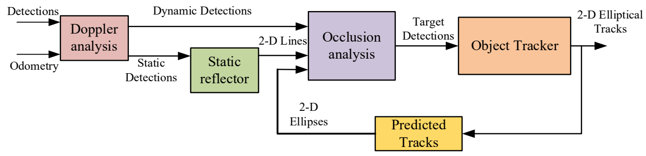

Fig. 1. Block diagram of the proposed system model.

The occlusion analysis stage evaluates the interaction between static objects and dynamic targets. It distinguishes true dynamic targets from occluded targets, estimating the presence of targets potentially hidden behind static objects based on their locations.

The Object Tracker utilizes a sophisticated model that accommodates the size and shape of the target, estimating its state over time, including position, velocity, and orientation. Predicted tracks are generated based on this estimated state, providing insights into the target's future trajectory and potential uncertainty.

To enhance robustness, the system conducts another occlusion analysis by predicting target locations and assessing potential occlusions with static objects. This iterative process aids in refining tracking accuracy and adaptability in dynamic highway scenarios.

Overall, this model integrates Doppler analysis, static clutter handling, and an extended object tracker to offer a comprehensive understanding of tracked objects, particularly in environments characterized by static clutter and potential occlusions.

As shown in Fig. 2, the tracking scenario uses an ego vehicle with a radar sensor and simulates passing vehicles.

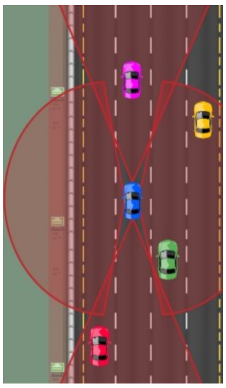

Fig. 2. Vehicle tracking in urban scenarios.

B. Design Parameters

The design parameters include (i) power density, (ii) radar cross-section (RCS), (iii) received signal power, (iv) maximum range, and (v) Doppler velocity.

(i) Power density: Antennas of radar focus the transmitted power P_t into a narrow beam using directive antennas with high gain G, as described in following equation, which significantly affects the power density received by the target at a specific range R [14],

$$P_d = \frac{P_t G}{4\pi R^2} \tag{1}$$

(ii) RCS: Radar cross section (RCS), also known as radar reflectivity σ, as described by the following equation, determines the power density reradiated back to the radar from a target [14].

$$P_{rad} = \frac{P_t G}{4\pi R^2} \cdot \frac{\sigma}{4\pi R^2} \tag{2}$$

(iii) Received signal power: The strength of the signal received by a radar P_r depends on two things: how much power hits the antenna in the first place, and how good the antenna is at capturing that power [14].

$$P_r = \frac{P_t G}{4\pi R^2} \cdot \frac{\sigma}{4\pi R^2} \cdot A_e = \frac{P_t G A_e \sigma}{(4\pi)^2 R^4} \tag{3}$$

(iv) Maximum range: The maximum target detection range R_{max} of a radar system is limited by the minimum detectable signal strength S_{min}. This occurs when the received signal power P_r from a target falls below S_{min}. Substituting S_{min} for P_r in equation (3) we get,

$$R_{max} = \left[\frac{P_t G A_e \sigma}{(4\pi)^2 S_{min}}\right]^{\frac{1}{4}} \tag{4}$$

This is the fundamental form of the radar range equation [14].

(v) Doppler velocity: Radars rely on the Doppler effect, which arises from an object's movement relative to the radar, to measure the rate of change in the object's distance. The Doppler theorem relates the radial velocity v, which is the component of an object's motion directed towards or away from the radar, to the maximum unambiguous Doppler velocity V_{max} are given as follows [14].

$$v = f_d \cdot \frac{\lambda}{2} \tag{5}$$

$$v_{max} = PRF \cdot \frac{\lambda}{4} \tag{6}$$

where, f_d = Doppler frequency shift, λ = wavelength, and PRF = pulse repetition frequency (sampling rate).

C. Mathematical Modeling

The proposed system model includes (i) range measurement of moving vehicle, (ii) Velocity measurement of moving vehicle, and (iii) yaw angle of moving vehicle.

(i) Range measurement: Target ranging is achieved by measuring the round-trip travel time T_{R_n} of the radar signal. Since electromagnetic waves propagate in free space at the speed of light $c = 3 \times 10^8\ m/s$, the target range R_n can be estimated using the following relationship [15]:

$$R_n = \frac{c . T_{R_n}}{2} \tag{7}$$

(ii) Velocity measurement: Leveraging the Doppler frequency shift phenomenon, we can measure the radial velocity V_n of a moving vehicle. The velocity of vehicle is as follows [16].

$$V_n = \Delta f_n . \lambda \tag{8}$$

where, Δf_n = Doppler frequency shift, and λ = wavelength.

(iii) Yaw Angle measurement: The yaw angle of vehicle is measured by the following equations [17], [18].

$$r_n = \sqrt{x_n^2 + y_n^2 + z_n^2} \tag{9}$$

$$\theta_n = \cos^{-1}\left(\frac{x_n}{r_n}\right) \tag{10}$$

where, (x_n, y_n, z_n) = position of vehicle in the Cartesian coordinates found by detection.

r_n = length of the line segment from the highest point (x_n, y_n, z_n) of vehicle to the radar and θ_n = azimuth angle of vehicle.

D. Object Tracking Techniques

(i) Point Object Tracker: Point-object trackers focus on identifying and following discrete objects in a scene. They typically rely on algorithms that detect and match points of interest (features) across frames. One common approach is the Kalman filter, which estimates a point object's state based on its previous state and measurements [19].

State Prediction:

$$x_{k|k-1} = Fx_{k-1|k-1} + Bu_{k-1} \tag{11}$$

State Update:

$$x_{k|k} = x_{k|k-1} + K_k\left(z_k - Hx_{k|k-1}\right) \tag{12}$$

where, $x =$ state vector, $F =$ state transition model, $B =$ control input model, $u =$ control vector, $K =$ Kalman gain, $z =$ measurement vector, and $H =$ observation model.

(ii) GGIW-PHD Tracker: The Gamma Gaussian Inverse Wishart Probability Hypothesis Density (GGIW-PHD) tracker is a method for tracking extended objects, which can occupy multiple measurements in a single frame. It models both the kinematic state and the shape of the objects, allowing for more accurate tracking of complex objects. The GGIW-PHD tracker is based on the following update equations [20].

PHD Prediction:

$$D_{k|k-1}(\xi_k) = \sum_{j=1}^{J_{k|k-1}} \mathcal{W}^j{}_{k|k-1}\mathcal{GGIW}\left(\xi_k; \zeta^j{}_{k|k-1}\right) \tag{13}$$

PHD Update:

$$D_{k|k}(\xi_k) = \sum_{P\angle Z_k}\sum_{W\epsilon P}\sum_{j=1}^{J_{k|k-1}} \mathcal{W}^{j,w}{}_{k|k}\mathcal{GGIW}\left(\xi_k; \zeta^{j,W}{}_{k|k}\right) \tag{14}$$

where, $D =$ intensity function, $J =$ number of components, $\mathcal{W} =$ weight of the j$^{\text{th}}$ component, $\zeta =$ density parameter of the j$^{\text{th}}$ component.

(iii) GM-PHD Tracker: The Gaussian Mixture Probabilistic Hypothesis Density tracker is a popular variant of the PHD filter that approximates the intensity function as a mixture of Gaussian components. The GM-PHD tracker is characterized by the following prediction and update steps [21].

PHD Prediction:

$$D_{k|k-1}(x) = \sum_{i=1}^{J_{k-1}} \mathcal{W}^i{}_{k-1}\,\mathcal{N}\left(x; m^i{}_{k|k-1}, P^i{}_{k|k-1}\right) \tag{15}$$

PHD Update:

$$D_{k|k}(x) = (1 - P_D)D_{k|k-1}(x) + \sum_{z\epsilon Z_k}\sum_{i=1}^{J_{k-1}} \mathcal{W}^i{}_{k|k-1}q^i{}_k(z)\mathcal{N}\left(x; m^i{}_{k|k}, P^i{}_{k|k}\right) \tag{16}$$

Where, $\mathcal{W} =$ weights of the Gaussian components, $\mathcal{N} =$ denotes the Gaussian distribution, $m =$ mean of the Gaussian components and $P =$ covariance of the Gaussian components, and $q =$ likelihood function for the measurements.

E. Classification Techniques of object detection

Doppler analysis differentiates between moving objects (positive or negative shift) and stationary clutter (zero shift) based on the reflected signal's frequency shift. Occlusion analysis using the 2-line intersection method further classifies ghost detections: static ghosts (reflections off static objects) are identified when the line segment from the sensor to a detected object intersects the boundary of a known static reflector, while dynamic ghosts (reflections off other moving objects) are revealed by a line segment from the sensor to a detected object intersecting the ellipse representing the track of another confirmed moving object. By using both Doppler analysis and occlusion analysis together, the system can tell the difference between static and moving ghosts, which makes radar-based object detection more accurate.

III. Performance Analysis

In this simulation, there is an ego vehicle that contains a radar sensor, and eight vehicles around the ego vehicle are simulated in the scenario.

A. Paramters of Radar Sensors and Different Tracker

In simulation, a total four radar sensors were used in the vehicle. The parameters of radar sensors are listed in Table 1.

Table 1. Parameter of the Radar Sensors

	Front-facing long-range radar	**Rear-facing long-range radar**	**Rear-left-facing short-range radar**	**Rear-right-facing short-range radar**
Range Limits, $[R_{min}\ R_{max}]$ (m)	[0 80]	[0 80]	[0 35]	[0 35]
Field Of View, $(\Delta\theta, \Delta\varphi)$	$(45°, 5°)$	$(45°, 5°)$	$(150°, 5°)$	$(150°, 5°)$
Range Resolution, $\Delta R\ (m)$	2.5	2.5	1.25	1.25
Range Rate Resolution, $\Delta v\ (ms^{-1})$	1	1	0.5	0.5
Center Frequency, $f_c(GHz)$	77	77	77	77
Bandwidth, $B\ (MHz)$	3	3	3	3
Peak Power, $P_t(watt)$	5000	5000	5000	5000
Transmitting Antenna Gain, $G_t(dB)$	20	20	20	20
Receiving Antenna Gain, $G_r(dB)$	0	0	0	0

In simulation, a three-difference tracker is used to evaluate their performance. The parameters of these trackers are listed in Table 2.

TABLE 2. PARAMETERS OF DIFFERENT TRACKER

Parameters	Point Object Tracker	GGIW-PHD Tracker	GM-PHD Tracker
Assignment Threshold	25	400	550
Extraction Threshold	-	0.70	0.80
Confirmation Threshold	3	0.85	0.95
Merging Threshold	-	40	40

B. *Tracking Performance of Three Object Tracker*

Fig. 3 shows the position tracking performance of three object trackers: a point tracker, the GGIW-PHD tracker, and the GM-PHD tracker. The figure shows the true position of a vehicle (represented as a solid line) alongside the tracked positions estimated by each tracker (shown as separate lines). This comparison allows us to evaluate the accuracy of each tracker by visually assessing how closely their estimated positions follow the actual vehicle trajectory.

While point-object trackers provide simplicity and speed, their accuracy is hampered by clutter. GGIW-PHD trackers excel in robustness against clutter and multiple targets, but their computational cost and model complexity can be high. GM-PHD trackers provide a balance, offering better robustness than point trackers with lower computational demands compared to GGIW-PHD trackers, making them a favorable choice for tracking point objects in challenging environments.

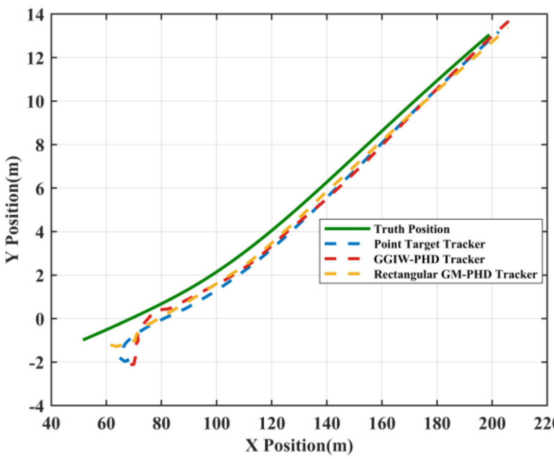

Fig. 3. Trajectory tracking performance.

Fig. 4 depicts the velocity tracking performance of the three object trackers for a vehicle with a constant true velocity of 27 m/s. The figure shows the true velocity over time (represented by a solid line), along with the tracked velocities estimated by each tracker (shown as separate lines).

This comparison reveals the effectiveness of each tracker in estimating the object's velocity. We observe that the GGIW-PHD tracker and GM-PHD tracker closely follow the true velocity, indicating their ability to accurately track the object's speed. In contrast, the point object tracker exhibits significant deviations from the true velocity, suggesting limitations in its ability to handle constant velocity motion.

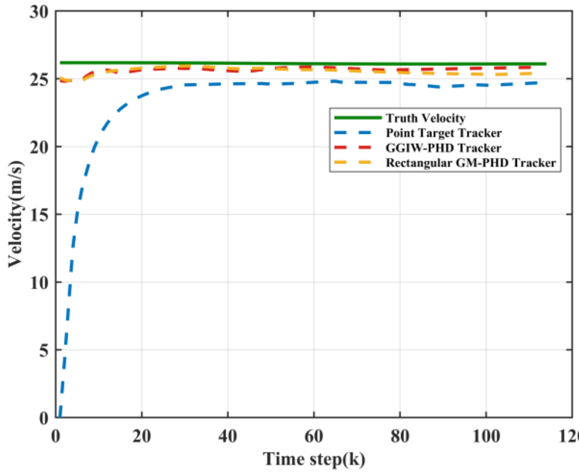

Fig. 4. Velocity tracking performance over time step.

Fig. 5 focuses on the yaw angle tracking performance of the three object trackers for a vehicle. The figure shows the vehicle's true yaw angle over time, as well as the tracked yaw angles estimated by each tracker.

This comparison highlights the ability of each tracker to estimate the vehicle's rotational motion. We observe that the GGIW-PHD and GM-PHD trackers track the yaw angle closely, suggesting their proficiency in capturing the vehicle's orientation changes. Conversely, the point object tracker struggles to follow the true yaw angle, exhibiting significant deviations in its tracking. This indicates limitations in the point object tracker's capability to handle rotational dynamics.

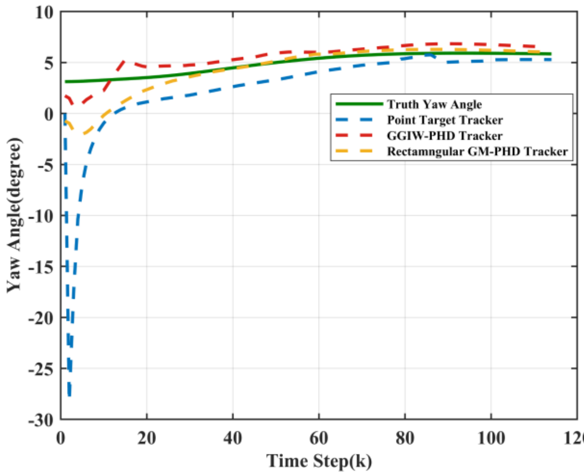

Fig. 5. Yaw angle tracking performance over time step.

Fig. 6 analyzes the number of vehicle tracks identified by each object tracker during the simulation. While all trackers successfully identified the eight vehicles, the point-object tracker exhibits the highest number of false and redundant tracks. This suggests that the point object tracker might be overly sensitive to noise or struggle with differentiating between vehicles and clutter.

In contrast, the GGIW-PHD tracker demonstrates a significant reduction in both false and redundant tracks compared to the point object tracker. This indicates a better balance between capturing all vehicles and minimizing false positives. The GM-PHD tracker achieves the lowest number of false and redundant tracks, suggesting the most accurate and efficient tracking performance among the three methods.

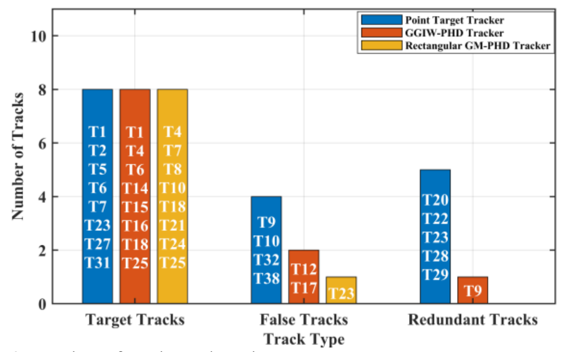

Fig. 6. Number of tracks and track type.

Fig. 7 compares the computational performance of the three object trackers. The figure likely depicts the average computation time required by each tracker to process a single frame.

The point object tracker, as observed, has the lowest computation time. This is likely due to its simpler design and fewer calculations involved in tracking objects. The GGIW-PHD tracker requires a moderately higher computation time compared to the point object tracker, suggesting a balance between tracking complexity and efficiency. Finally, the GM-PHD tracker demonstrates the highest computational cost. The GM-PHD tracker's sophisticated algorithms and ability to handle complex tracking scenarios with higher accuracy could account for this.

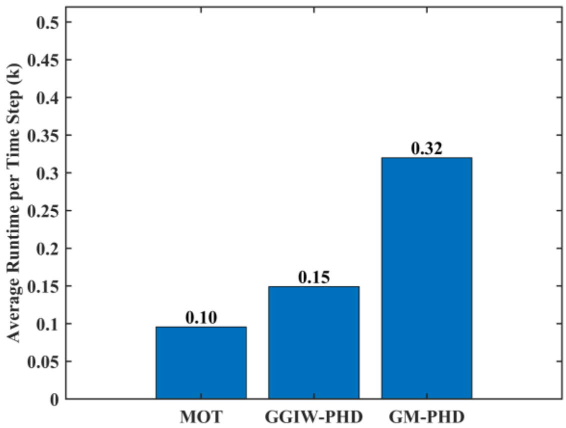

Fig. 7. Computational performance comparison.

C. Classification accuracy of detection

The number of detections of true information that remain in the scenario are enlisted in Table 3.

TABLE 3. TRUE INFORMATION

True Information	Number of Detection
Targets	1969
Ghost (S)	3155
Ghost (D)	849
Environment	27083
Clutter	138

The performance of the radar detection classification algorithm was evaluated using a confusion matrix, which is shown in Fig. 8. This matrix compares the true classifications (rows) of radar detections with the algorithm's predicted classifications (columns). The analysis revealed high accuracy for target detection, with over 91.4% correctly classified. However, a small percentage of true targets were misclassified as ghosts originating from static object reflections (represented by a non-zero value in the second element of the first row). Ghost detections also showed some misclassification. The system mistakenly classified approximately 3.16% of ghosts from static reflections and 17.55% of ghosts from dynamic reflections as targets. It's important to note that the current algorithm focuses solely on classifying detections and doesn't handle false alarms or clutter within the scene. Consequently, the confusion matrix shows zero entries in the "false alarm" column.

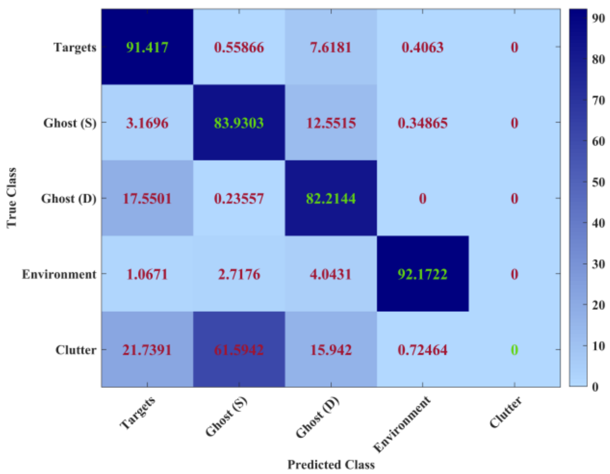

Fig. 8. Percentage True vs. Predicted Confusion Matrix.

The precision, recall, and F1 score of the classification are listed in Table 4.

TABLE 4. PRECISION, RECALL, F1 SCORE OF CONFUSION MATRIX

Class	Precision (%)	Recall (%)	F1-Score (%)
Target	91.417	76.0135	83.01
Ghost (S)	83.93	76.048	79.795
Ghost (D)	82.214	29.5637	43.489
Environment	92.172	99.92	95.89

IV. CONCLUSION

This paper investigated the performance of various object tracking algorithms for multi-object tracking (MOT) using radar data. The primary focus was on comparing the point object tracker, the GGIW-PHD tracker, and the GM-PHD tracker. The analysis revealed a trade-off between computational complexity and tracking accuracy. The point object tracker offered the lowest computational demand but lacked the ability to estimate dimension and was susceptible to errors when objects were in close proximity. In some scenarios, the GGIW-PHD tracker provided a balance between efficiency and accuracy, offering dimension estimation with potentially similar or slightly better position tracking compared to the GM-PHD tracker. However, its assumptions about measurement distribution could influence its performance. The GM-PHD tracker delivered the most accurate state estimation for all variables (position, velocity, and yaw) but demanded the most computational resources.

REFERENCES

[1] M. Rath, “Smart traffic management system for traffic control using automated mechanical and electronic devices,” in *Proc. International conference on mechanical, materials and renewable energy*, India, 2018.

[2] S. Gupte, O. Masoud, R. Martin, and N. Papanikolopoulos, “Detection and classification of vehicles,” *IEEE transactions on intelligent trans portation systems,* vol. 3, no. 1, pp. 37–47, 2002.

[3] M. G. Moazzam, M. R. Haque, and M. S. Uddin, “Image-based vehicle speed estimation,” *Journal of computer and communications,* vol. 7, no. 1-5, p. 1, 2019

[4] I. H. Shibly, M. M. Zaman, M. S. Hossain and M. M. S. Hasan, "Performance Analysis of Adaptive Cruise Control Using Frequency Modulated Continuous Wave Radar Under Rain Clutter," *2023 26th International Conference on Computer and Information Technology (ICCIT)*, Cox's Bazar, Bangladesh, 2023, pp. 1-5, doi: 10.1109/ICCIT60459.2023.10441169.

[5] F. Bafghi and B. Shoushtarian, “Multiple-vehicle tracking in the highway using appearance model and visual object tracking,” in *Proc. 11th Iranian and the first international conference on machine vision and image processing,* Isfahan, Iran, 2020.

[6] M. A. Adnan, N. I. Zainuddin, N. Sulaiman, and T. B. H. T. Besar, “Vehicle speed measurement technique using various speed detection instrumentation,” in *IEEE Business Engineering and Industrial Applica tions Colloquium (BEIAC),* Malaysia, 2013.

[7] M. Abdelsalam and T. Bonny, “Iov road safety: vehicle speed limiting system,” in *Talal Bonny*, Sarjah, UAE, 2019.

[8] P. Jiwattanakulpaisarn, K. Kanitpong, and P. Suriyawongpaisal, “Ef fectiveness of speed enforcement in thailand: Current issues, need for changes and new approaches,” *Transport and communications bulletin for Asia and the Pacific*, vol. 1, no. 79, p. 41, 2009.

[9] U. Gupta, U. Kumar, S. Kumar, M. Shariq, and R. Kumar, “Vehicle speed detection system in highway,” *International research journal of modernization in engineering technology and science*, vol. 4, no. 5, p. 406, 2022.

[10] G. D. Sullivan, K. D. Bake, A. D. Worrall, C. I. Attwood, and P. R. Remagnino, “Model-based vehicle detection and classification using orthographic approximations,” *Image and vision computing*, 1996.

[11] R. Mobus and U. Kolbe, “Multi-target multi object tracking, sensor fusion of radar and infrared,” in *IEEE intelligent vehicles symposium,* Parma, Italy, 2004.

[12] R. A. MacLachlan and C. Mertz, “Tracking of moving objects from a moving vehicle using a scanning laser range finder,” in Proc. *IEEE intelligent transportation systems conference*, Canada, 2006.

[13] O. Masoud and N. Papanikolopoulos, “Detection and classification of vehicles,” in *IEEE transactions on intelligent transportation systems, Minneapolis*, 2002.

[14] M. I. Skolnik, *Introduction to Radar Systems*, 3rd ed., New York: McGraw-Hill, 2001.

[15] S. S. Islam, M. M. Sakib and M. S. Hossain, “Performance Analysis of Scan Ra ar Beamforming for the Detection of Multiple Targets,” *2023 6th International Conference on Electrical Information and Communication Technology (EICT)*, 2023, pp. 1-6.

[16] S. S. Islam, M. S. Hossain, M. F. Shahriar, M. A. Rouf and M. M. Sakib, “Performance Investigation of Phased Array Scan Radar System for Multi-Target Detection,” *2023 26th International Conference on Computer and Information Technology (ICCIT)*, 2023, pp. 1-6.

[17] S. S. Islam, M. S. Hossain, M. F. Shahriar, M. A. Rouf, S. N. Kakoli and M. S. Jafor, “Assessment of Phased Array Radar Performance in Multi-Object Detection for Enhanced Surveillance,” *2024 3rd International Conference on Advancement in Electrical and Electronic Engineering (ICAEEE)*, 2024, pp. 1-6.

[18] S. S. Islam, M. F. Shahriar, S. N. Kakoli, S. M. Al Razi and Z. I. Purno, “Efficient Multiple Moving Object Detection and Tracking by Uniform Rectangular Array-Based Surveillance Radar System,” *2024 6th International Conference on Electrical Engineering and Information & Communication Technology (ICEEICT)*, 2024, pp. 752-757.

[19] R. E. Kalman, "A new approach to linear filtering and prediction problems," *Transactions of the ASME–Journal of Basic Engineering*, vol. 82, no. Series D, pp. 35-45, Mar. 1960.

[20] J. Sjudin, M. Marcusson, L. Svensson and L. Hammarstrand, "Extended Object Tracking Using Sets Of Trajectories with a PHD Filter," *2021 IEEE 24th International Conference on Information Fusion (FUSION)*, Sun City, South Africa, 2021, pp. 1-8, doi: 10.23919/FUSION49465.2021.9626994.

[21] B. Vo and W. K. Ma, "The Gaussian Mixture Probability Hypothesis Density Filter," *IEEE Transactions on Signal Processing*, vol. 54, no. 11, pp. 4091-4104, Nov. 2006.